AUTOMATIC ITERATION ON VISCOUS DAMPING FOR OPTIMAL SRP WELL

Victoria Pons, Ph. D., and Jeremy Gomes

WellWorx Energy

ABSTRACT

A new methodology for automatic iteration on viscous damping enhanced with state-of-the-art pump fillage, fluid load lines and valve openings and closing calculation is presented. Field results showing the impact of the methodology in diagnosing downhole conditions, improving inferred production, fluid level, pump intake and horsepower calculations are shown.

The new approach uses a wave equation model with iteration on viscous damping paired with a traveling valve and standing valve calculation. Pump fillage and fluid load lines are calculated, which enables calculation of mechanical friction. The iteration uses a bisection method-like algorithm, which speeds up the convergence and removes the algorithm's dependence on horsepower convergence criteria and other fluid and well variables.

In sucker rod pumped wells, efficiency and control of the entire system is ruled by elasticity, viscous friction and mechanical friction. Elasticity comes from the elastic behavior of the rod string and the propagation of stress waves due to the cyclic pumping operation traveling up and down the rod string at the speed of sound. Mechanical friction results from the rod string, couplings or pump coming in contact with the tubing. Viscous friction originated from produced fluid imparting a viscous force on the outer diameter of the rod string during operation. Those three factors are the basis for the calculation of downhole data from surface data to enable optimization and better control of sucker rod pump applications. Neglecting viscous friction leads to erroneous downhole data.

Very often, downhole cards have an over loop appearance which is physically impossible when considering pumping unit dynamics. This is due to the viscous force not being adjusted properly. Also, what can be mistaken from mechanical friction can be in fact completely removed from downhole data using appropriate viscous adjustment. Finally, operators traditionally overestimate their inferred production from the extra fictive load that is present on a poorly viscous friction adjusted card. The field data results presented in this paper show this new approach eradicates all these issues to deliver accurate and truthful downhole data.

The new approach iterates on the optimal damping factor for both the upstroke and downstroke for every stroke. Currently, most controllers utilize a manually adjusted damping factor, which leads to the damping factor not being adjusted for every stroke. Repercussions of this include overestimation of inferred production, overlooping phenomenon and appearance of excessive mechanical friction.

INTRODUCTION

In Sucker Rod Pumped wells, the circular motion at the surface is translated in a vertical motion of the rod string, effectuating the pump. The movement of the rod string is impeded by three phenomena: elasticity, viscous friction, and mechanical friction.

The rod string is composed of thousands of feet of rods made of steel, fiberglass, and other material. At each stroke, the rod string lifts the weight of the rod string elements below as well as the weight of the lifted fluids. During the pumping cycle, the rods string experiences cyclic compression and tension as the rods move up and down thousands of feet. This phenomenon creates stress waves that travel up and down the rod string at the speed of sound. This is called Elasticity. This removes energy from the system as stress waves coming from two different points can coincide to create compression in the rod string and therefore buckling.

Secondly, the fluid lifted to the surface imparts a viscous force on the outer diameter of the rod string slowing down its progression. Viscous forces are proportional to the velocity of the rod string, which means that pumping fast accentuates viscous forces and introduced viscous dynamics in the downhole data, whereas pumping slow will reduce the dynamics observed within a stroke, cf. [9, 10, 14].

Finally, mechanical friction results from the lateral movement of the rod string and its contact with either the tubing, or the pump. Mechanical friction is issued from contact, see [5, 8, 9, 11]. This happens mostly due to deviation but can also happen in cases of paraffin or other solids. Mechanical friction can be seen as a pinpoint for the rod string where movement is either stopped or slowed down due to a physical barrier (i.e. the tubing, pump or paraffin). The model presented in this paper only considers viscous forces. WellWorx has also developed a Deviated Diagnostic model, which will be presented in a later paper. Both methods are available in the Ken Well Manager in summer 2024.

Traditionally, the wave equation is used to calculate downhole data from surface data, see [1, 2, 3, 4, 6, 7, 10, 12, 13].

In the majority of methods available to the operator for downhole data calculation and automation hardware and software, viscous damping is a set value, where a coefficient might get adjusted whenever the field technician has time and spends time optimizing and analyzing the well. In reality, viscous damping is a dynamic quantity for two major reasons. The first reason is that as mentioned above viscous friction is proportional to the velocity of the rod string. This means that operating conditions will greatly affect the presence of viscous friction in the system. Secondly, viscous friction depends on the amount of fluids being lifted to the surface, which varies greatly during the pumping cycle. As the well pumps off, less fluids are being produced, therefore less viscous friction in the system and therefore the damping factor should be lowered. This requires constant adjustment for the donwhole data to be accurate, cf. [10, 14].

With most of the industry being now satisfied with erroneous results from ill-adjusted damping factors, downhole data that is either overdamped, where a loop is present on the right-hand side of downhole card as shown in Figure 1A or underdamped characterized by a fat downhole card as shown in Figure 1B, are all too common in our industry. An optimally damped downhole card is displayed in Figure 1C.

The first case displays a downhole card, which can’t exist due to the physical constraints of the pumping unit, so the data has been altered to the point that it is now falsified. In the second case, the downhole card is blown up, which causes all values from fluid load, gross stroke and netstroke to be grossly distorted.

In this paper, a method is presented to properly account for viscous friction present in the system using an iterative process which iterates on an upstroke and downstroke damping factors independently for every stroke of a well. The presented iteration does not depend on values such as fluid level or other time-sensitive user inputs and instead uses a mathematical process to guarantee proper convergence and viscous friction handling.

Results showing the stability and accuracy of the method are presented.

In the following section, details on the methods and procedures employed are presented.

METHODS & PROCEDURES (RENAME)

A. Rod Pumps & Wave Equation

When the assumption is made that the rod string does not move laterally, i.e. the rod string only moves up and down and effects of deviation are neglected, the rod string can be compared to an ideal slender bar and the propagation of the stress waves becomes a one-dimensional phenomenon. Under this assumption, one can use the wave equation to model the propagation of the stress waves in the rod string, see [9, 14].

The condensed one-dimensional wave equation reads:

$$v^2 \frac{\partial^2 u}{\partial x^2} - D \frac{\partial u}{\partial t} = \frac{\partial^2 u}{\partial t^2}, \quad (1)$$

where the acoustic velocity is given by: $v = \sqrt{\frac{144Eg}{\rho}}$.
The first term in the equation represents elasticity; the second term represents the viscous damping force, while the last represents the system's acceleration.

As can be seen from the negative sign in front of the damping force, the goal of the damping term is to remove energy from the system to mimic the energy lost due to viscous forces. As mentioned, mechanical friction is ignored for this model. This model uses a finite difference method solution to the wave equation.

Viscous Damping represents energy we are removing from the wave equation which mimics the energy lost due to viscous friction during pumping. Conditions are very different between the upstroke and downstroke, i.e., due to the direction of the fluid flowing with or against the rods. The same damping factor cannot be used for both upstroke and downstroke. As the wells pumps off, viscous friction decreases, and different values for damping are needed. Therefore, a separate damping factor should be used for the upstroke than for the downstroke.

In practice, calculating damping factors is not a reliable method for great accuracy. Iterating on upstroke and downstroke damping factors is preferred and much more accurate, see [10, 14].

B. Key control parameters

Key control parameters must be extracted from downhole position and load data to optimize and efficiently control a sucker rod-pumped installation, as shown in Figure 2.

These key control parameters include:

- Fluid load - F0 – vertical span of the downhole card
- Net stroke – NS – refers to the portion of the plunger travel that contains fluid, i.e. pump fillage PF
- Traveling valve opening and closing
- Standing valve opening and closing

The above quantities are essential in inferred production calculation as well as slippage and oil shrinkage calculation. Inferred production is an important KPI to measure efficiency of installation.

Results showing the impact of WWX's calculations on the above KPI are discussed in the results section of this paper.

C. Fluid Load, Fluid Level and Pump Intake Pressure calculation

The fluid load is the difference between the upstroke and downstroke fluid load lines, as in (2).

$$F0 = F0UP - F0DN = F0_{TRUE}. \quad (2)$$

Most companies calculate fluid load F0 as the difference in load values, or load range (see (3)), but this practice produces incorrect results especially if the well is deviated and mechanical friction is present in the well bore.

$$F0^* = \max(Load) - \min(Load) \approx F0_{EFF}. \quad (3)$$

In the deviated case, the load range includes all the mechanical friction on both the upstroke and downstroke, meaning that the fluid load and the load range can be very different values according to (4) and (5).

$$F0^* = F0 + Upstroke\ Mechanical\ Friction + Downstroke\ Mechanical\ Friction, \quad (4)$$

$$F0^* \neq F0 \text{ and } F0^* \gg F0. \quad (5)$$

If F0* ($\approx F0_{EFF}$) is used to calculate Fluid level, then the fluid level might be calculated as negative which of course is not possible. In turn, all other calculations using fluid level will be erroneous such as hydraulic horsepower and production rate.

To avoid this, the $F0_{TRUE}$ can be calculated by estimating the upstroke and downstroke mechanical friction and removing it from F0* as shown in the Figure 2. Using $F0_{TRUE}$ affords the operator a true picture of the fluid being moved and an opportunity to understand and accurately estimate how much production is still available in the wellbore.

D. Inferred Production Calculation

Inferred production allows the operator to estimate how much fluid and gas is being produced by the well based on the pump fillage of the downhole data, oil shrinkage and oil slippage. Accurate calculation of pump fillage is critical for optimal results and efficiency of pumping operations. Pump fillage can be difficult to calculate due to the many different downhole conditions that can happen in the well.

Correct calculation of valve openings and closings is also essential to the accurate calculation of the netstroke and the proper estimation of slippage but can be very challenging to calculate correctly due to the dynamic nature of the DHC. Pump fillage and netstroke are moving targets as the well cycles from full to pumped off conditions. WWX new state of the art method accurately solves for NS, PF and valve openings and closings, as shown in Figures 2, 5, 7, 9, 11, 13, 15.

E. Iterative Process

Note that the iterative process described in this paper is agnostic to the type of method used to solve the wave equation. However, proper care should be taken to ensure that damping factors are within bounds depending on the method used. For this reason, this paper will focus on the iteration process and not on the method of solving the wave equation. Examples of methods employed to solve the wave equation can be found in [1, 2, 6, 9, 10].

Figure 3 shows a flowchart of the proposed iterative process.

As can be seen in the flowchart displayed in Figure 3, the iteration starts with an initialization step with an upstroke damping factor of 0.25 and a downstroke damping factor of 0.5. Damping factor should be strictly less than 1 and greater than 0.

In this first step, the downhole data is calculated along with several control parameters as well as the position for the traveling valve and standing valve opening and closing. Calculated parameters are shown

in Figure 2. These include effective fluid load lines (F0*) and true fluid load lines (F0) as well as pump fillage PF, netstroke NS, standing valve opening (SVO), standing valve closing (SVC), traveling valve opening (TVO) and traveling valve closing (TVC).

Convergence of the algorithm is achieved by two different methods. If a current fluid level value is available and there is no mechanical friction present in the well, the algorithm will converge when the pump horsepower is equal to the hydraulic horsepower. Unfortunately, most fluid level values input in controllers can be several weeks or months old and most definitely do not represent the current well condition.

To ensure convergence a secondary method is implemented which compares the upstroke and downstroke fluid load with the mean of the upstroke and downstroke points between the previously calculated valve openings and closings.

This asserts if the downhole data is overdamped, underdamped, or damped correctly.

The innovative part of this method is the selection of the iterated damping factors, using a bisection-like approach. If the downhole data is found to be overdamped, this means that the damping factor should be reduced. The updated damping factor to be used in the following iteration is taken to be the middle of the lower interval.

For example, if the upstroke damping factor after the initialization stage needs to be reduced, the new value will be the middle of the interval (0, 0.25), i.e. 0.125. Similarly, if the upstroke damping factor needs to be increased, the new value will be the middle of the interval (0.25, 1), i.e. 0.625. In the following iteration, if the upstroke damping factor needs to be decreased, the middle of (0.25, 0.625) will be chosen whereas if the damping factor should be increased, the middle of the (0.625,1) will be taken.

The process repeats until either the method converges or the difference between two consecutive damping factors falls below tolerance.

In other iterative methods, inaccurate customer input values such as tubing head pressure, fluid level and tubing gradient causes the iterative process to fail when mechanical friction is present in the well. Unfortunately, in today's time, the great majority of wells pumped using reciprocation rod lift are not vertical and contain moderate to significant deviation. This means that such iterative process is bound to failure, leaving data underdamped and calculating negative fluid level and incorrect pump intake pressure values.

Using the iterative process described above, dependance on user input values is removed. The correct selection of damping factors becomes a mathematical process.

Moreover, the bisection-like method offers a much faster convergence reducing the number of needed iterations to a handful compared to double digits in other methods. This is done by the ability to quickly zoom into the correct values for the upstroke and downstroke damping factor.

In the next section, results are presented and discussed.

RESULTS & DISCUSSION

In this section, results from three wells will be presented. For each example, calculated downhole card is compared to the downhole data generated from a fixed damping factor method from controller data. These examples represent examples where the data is under-damped. Over-damped cases are not considered. In the case of over-damped, the diagnosis is obvious from an over loop of the card and therefore disregarded for this paper.

Figure 4 shows the graphical representation of surface data (in green) along with the graphical representation of downhole data, first generated from the controller using a fixed damping factor (in black), the other generated using a finite difference solution to the wave equation and the proposed Iteration on Damping (ITEDAMP) (in blue).

The downhole cards displayed in Figure 4 show a gas interference condition from the sloped appearance of the downhole card on the lower right-hand side of the downhole card. As evident from the fat nose on the downhole card, a lot of friction is present on the upstroke and downstroke. The friction as mentioned above could be attributed to viscous or mechanical friction. Even industry experts would not be able to ascertain which type of friction is present in the well without further analysis. There is a slight difference in orientation of the two downhole cards, but this is not of importance here and can be ignored.

Figure 5 shows the results from the WellWorx proprietary Diagnostic Model. The figure shows the downhole card along with the traveling valve openings (blue) and closings (green) as well as the standing valve openings (pink) and closings (red). Also, represented is the pump fillage or netstroke value in the form of a vertical green line. Used in the iteration on damping are the true and effective upstroke (red) and downstroke (blue) fluid load lines.

The damping factor used to compute the downhole card in Figure 5, was intentionally set to a lower value to match the results coming out of the controller in an effort to show the differences in computed values between an under-damped downhole data set and an ideal or optimally damped downhole data set.

Figure 6 and Figure 7 show the same type of graphs but this time with downhole data set computed from the Iteration on Damping finite difference solution (ITEDAMP). As can be seen by Figure 6, all the friction has been removed from the downhole data using the viscous iteration on damping. This means that the friction present in this well is of viscous nature only and very little due to mechanical friction. The resulting downhole card is a lot skinnier than the fixed damping example. Table 1 shows the well parameters as well as calculated horsepower for both the polished rod and downhole card, netstroke and production rate. With these quantities it is possible to calculate the amount of horsepower or energy lost to friction as well as the amount of production that was overestimated over the course of a day and over the course of a month.

As can be seen in Table 1, Well 1 has a surface stroke of 126.0 inches and a pumping speed of 12.55 SPM. The calculated netstroke is 54 .52 inches for the ITEDAMP card and 62.81 inches for the under-damped fixed damping controller card. The ideally damped card shows a fluid load of 5453 lbs. and load range of 7870 lbs. compared to 7164 lbs. and 10498 lbs. for the fixed damping factor card. The polished rod horsepower for Well 1 for this stroke is 33.03 HP, the calculated pump horsepower for the ideally damped card is 15.11 HP compared to 30.34 HP. This means that in the case of the under-damped card, the program erroneously attributes only 2.69 HP of energy lost to viscous friction compared to the actual 17.92 HP lost in the case of the ideally damped card.

For this example, any calculation that uses either the fluid load or the load range will also be severely off, due to a fluid load difference of 1711 lbs. and load range difference of 2628 lbs. from estimated to actual. This includes calculation for pump intake pressure and fluid level calculations.

The difference in netstroke values calculated in each case can have a big impact on the production rate calculated by the controller or software. This depends on the pumping speed, the netstroke, and plunger diameter. As can be seen in the last row, production was overestimated by 47.81 BPD, which adds up to 1,434 BPD in a month.

Figures 8-11 show the same figures as for Well 1 but for a second example well, Well 2. Figures 8 and 9 show the results in the under-damped case associated with the fixed damping controller card. Figures 10 and 11 show the results of the iteration on damping for Well 2.

This stroke example from Well 2 shows a pumped off downhole card as is evident by the sharp drop in load values in the middle of the downhole card on the downstroke. The card also has a very fat nose, which is indicative of friction of either viscous or mechanical nature. Figures 10 and 11, show downhole cards with the friction on the upstroke and downstroke mostly removed. When adjusting the damping factor for downhole data, it is important to maintain a flat appearance on both the upstroke and downstroke. The iteration on damping removed all the viscous friction present in the well, the left-over friction can be attributed to mechanical friction and can only be removed with a deviated diagnostic method. The nature of the two types of friction being vastly different means that mechanical friction cannot be removed by adjusting the viscous damping factor.

According to Table 2, the surface stroke for Well 2 is 366.0 inches. Well 2 has a pumping speed of 3.12 SPM. The calculated netstroke is 152.08 inches in the case of the ideally damped downhole card versus 153.67 inches in the case of the under-damped card. This might not seem much and does not have a huge effect at this low speed, this is after all a long stroke unit. However, this creates a difference of 2 barrels per day in over-estimated production rate, which adds up over one month to 60 BPD.

Additionally, the polished rod horsepower for Well 2 is 17.13 HP with a pump horsepower of 10.57 HP in the case of the optimally damped case versus 15.81 HP for the under-damped case. This means that in the under-damped case 1.32 HP was attributed to viscous energy losses when actually the real value is 6.56 HP.

For this example, pump intake pressure and fluid level calculations will be off due to a fluid load difference of 702 lbs. and load range difference of 1184 lbs. from estimated to actual.

Figures 12-15 are similar to the two previous examples except for Well 3. Figures 12 and 13 represent results for the under-damped fixed damping controller data while Figures 14 and 15 show data from the results of the iteration damping for Well 3. As can be seen in Figures 14 and 15, there is a big discrepancy in the downhole data calculated with the iteration on damping versus the under-damped case. Figure 15 shows a much skinnier card as well as true and effective fluid load lines that we are within tolerance of each other.

As can be seen in Table 3, Well 3 has a surface stroke length of 192 inches and a pumping speed of 6.99 SPM. The calculated netstroke for the optimally damped card is 162.33 inches compared to 162.89 inches for the under-damped case. Notice that in this example the difference in netstroke is not very big, but due to the faster pumping speed compared to the last example, this still adds up to 2 BPD or 60 barrels per month of over-estimated production.

The fluid load and load range for the ideally damped card are 4706 lbs. and 5443 lbs. compared to 5015 lbs. and 6644 lbs. for the under-damped example. For this well, the polished rod horsepower is 19.45 HP. In the ideally damped case, the pump horsepower is calculated to be 15.03 HP compared to 18.50 HP for the under-damped case. This means that, in reality 4.42 HP of work is lost to viscous friction compared to the 0.95 HP erroneously estimated in the fixed damping case.

For this example, pump intake pressure and fluid level calculations will be off due to a fluid load difference of 312 lbs. and load range difference of 1201 lbs. from estimated to actual.

In the next section, conclusions are presented, followed by references and tables& Figures.

CONCLUSIONS

Properly adjusting the viscous damping factors can have a big impact on properly calculating production rate and estimating energy lost to viscous forces.

As the pumping speed increases, it becomes more and more important to properly account for the viscous friction as viscous friction is proportional to the velocity of the rod string. As a well is pumped faster, any discrepancy or error in calculating downhole data such as under or over-estimating friction will have a snowball effect on production rate, horsepower calculation and many other calculations central to well optimization.

Incorrectly damped downhole data cannot yield correct control variables and can compromise the efficiency and return on investment for an installation. If the fluid load is over or under-estimated, fluid level calculations will be wrong. Erroneous fluid level estimates can cause the operator to mis-operate the well and lose potential production.

When operators are responsible for thousands of wells at one time, automatic iteration on viscous damping ensures that the appropriate amount of viscous energy is removed from the system. Correctly damped downhole data yields accurate inferred production and system efficiency and allows for an enhanced more accurate control of the pumping unit installation.

REFERENCES

1. Ehimeakhe, V.: “Comparative Study of Downhole Cards Using Modified Everitt-Jennings Method and Gibbs Method”, Southwestern Petroleum Short Course 2010.
2. Everitt, T. A. and Jennings, J. W.: “An Improved Finite-Difference Calculation of Downhole Dynamometer Cards for Sucker-Rod Pumps,” paper SPE 18189 presented at the 63rd Annual Technical Conference and Exhibition, 1988.
3. Gibbs, S. G., and Neely, A. B.: “Computer Diagnosis of Down-Hole Conditions in Sucker Rod Pumping Wells,” JPT (Jan. 1996) 91-98; *Trans.*, AIME,237
4. Gibbs, S. G.: “A Review of Methods for Design and Analysis of Rod Pumping Installations,” SPE 9980 presented at the 1982 SPE International Petroleum Exhibition and Technical Symposium, Beijing, March 18-26.
5. Gibbs, S. G.: “Design and Diagnosis of Deviated Rod-Pumped Wells”, SPE Annual Technical Conference and Exhibition, Oct 6-9, 1991, Dallas, USA.
6. Gibbs, S.G.:” Method of Determining Sucker-Rod Pump Performance,” U.S. Patent No. 3,343,409 (Sept. 26, 1967).
7. Knapp, R. M.: “A Dynamic Investigation of Sucker-Rod Pumping,” MS thesis, U. of Kansas, Topeka (Jan. 1969).
8. Lukasiewicz, S. A.: “Dynamic Behavior of the Sucker Rod String in the Inclined Well”, Production Operations Symposium, April 7-9, 1991, Oklahoma City, Oklahoma, USA.
9. Pons, V., “Vertical vs. Deviated wells: Balance of Forces and Equations”, 2021 SouthWestern Petroleum Short Course, Lubbock TX.
10. Pons-Ehimeakhe, V, “Modified Everitt-Jennings Algorithm, with Dual Iteration on the damping Factors”, SouthWestern Petroleum Short Course, April 2012, Lubbock TX.
11. Pons-Ehimeakhe, V*, Implementing Coulombs Friction for the Calculation of Downhole Cards in Deviated Wells*, SouthWestern Petroleum Short Course, 18-19 April 2012, Lubbock, Texas, USA.
12. Schafer, D. J. and Jennings, J. W.: “An Investigation of Analytical and Numerical Sucker-Rod Pumping Mathematical Models,” paper SPE 16919 presented at the 1987 SPE Annual Technical Conference and Exhibition, Dallas, Sept. 27-30.
13. Snyder, W. E.: “A Method for Computing Down-Hole Forces and Displacements in Oil Wells Pumped With Sucker Rods,” paper 851-37-K presented at the 1963 Spring Meeting of the API Mid-Continent District Div. of Production, Amarillo, March 27-29.
14. Takács, G.: “Sucker-Rod Pumping Manual.” PennWell, 2002.

FIGURES & TABLES

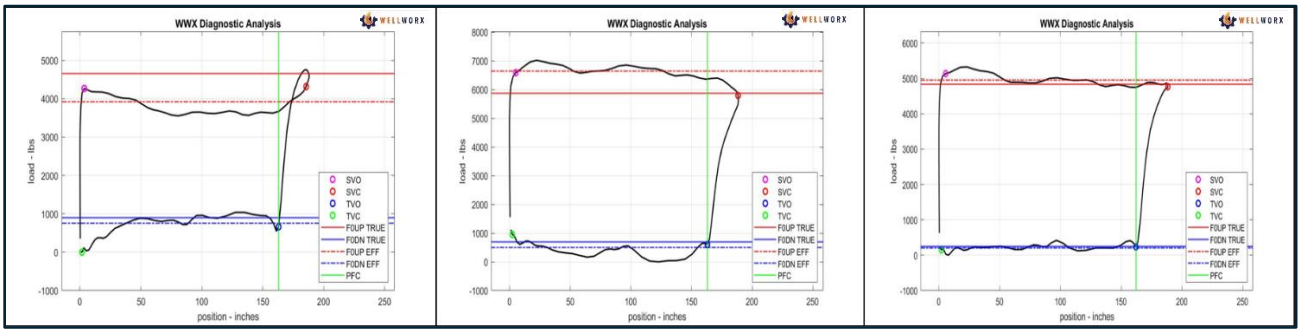

Figure 1: 1A (left) Overdamped downhole card, 1B (middle) Underdamped downhole card, 1C (right) Optimally damped downhole card.

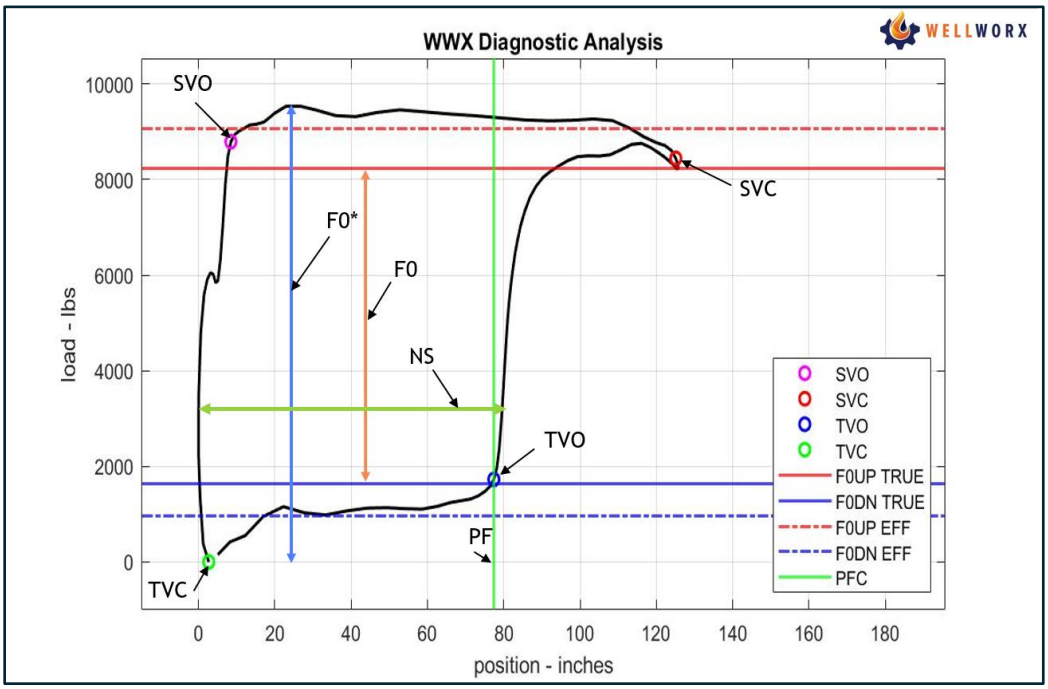

Figure 2: WellWorx Diagnostic Results.

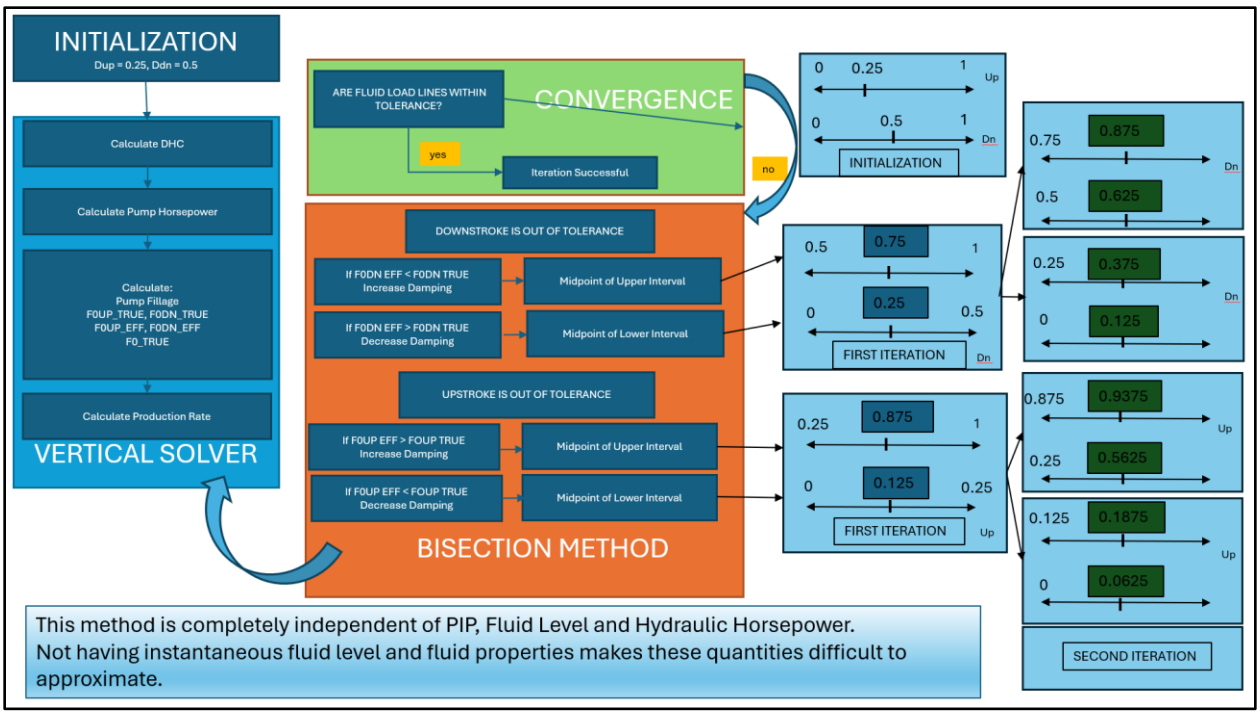

Figure 3: Flowchart of proposed iterative process.

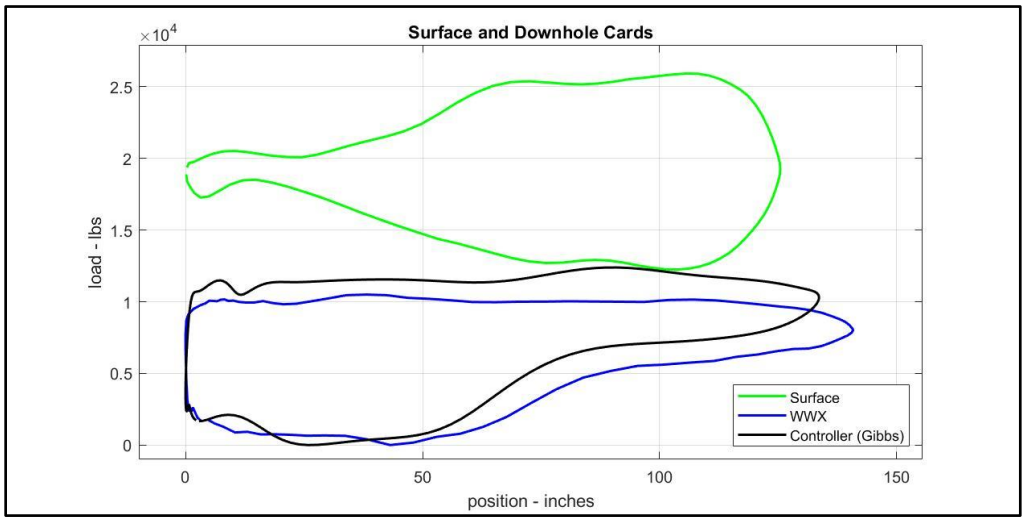

Figure 4: Comparison of results of Iteration on Damping with fixed damping controller method and surface data for Well 1 with low damping factor to match controller output.

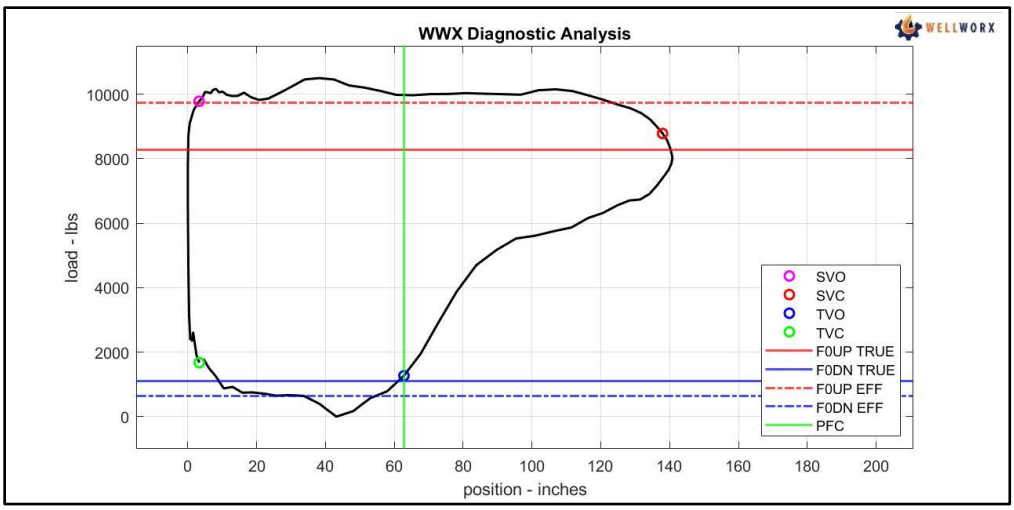

Figure 5: Results of WWX Diagnostic Analysis for Well 1 with low damping factor to match controller output.

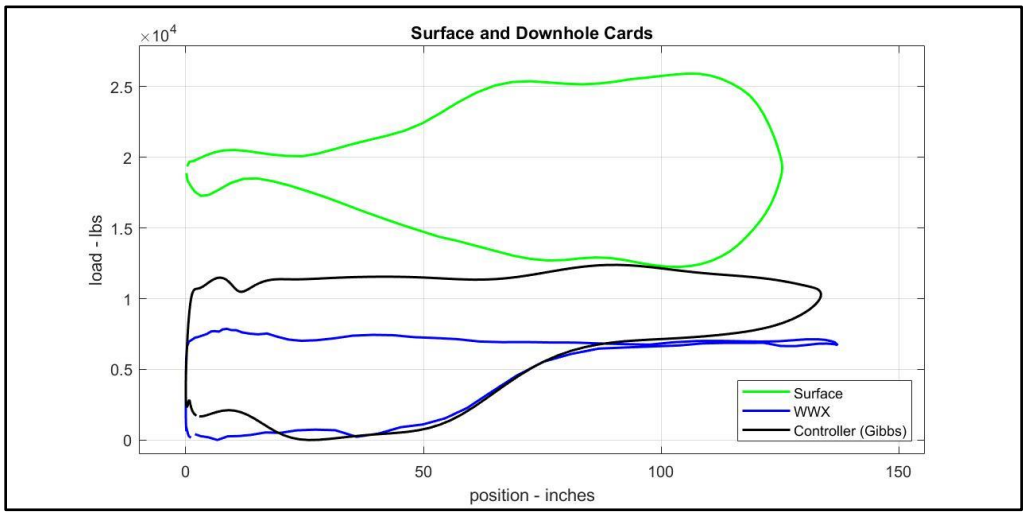

Figure 6: Comparison of results of Iteration on Damping with fixed damping controller method and surface data for Well 1.

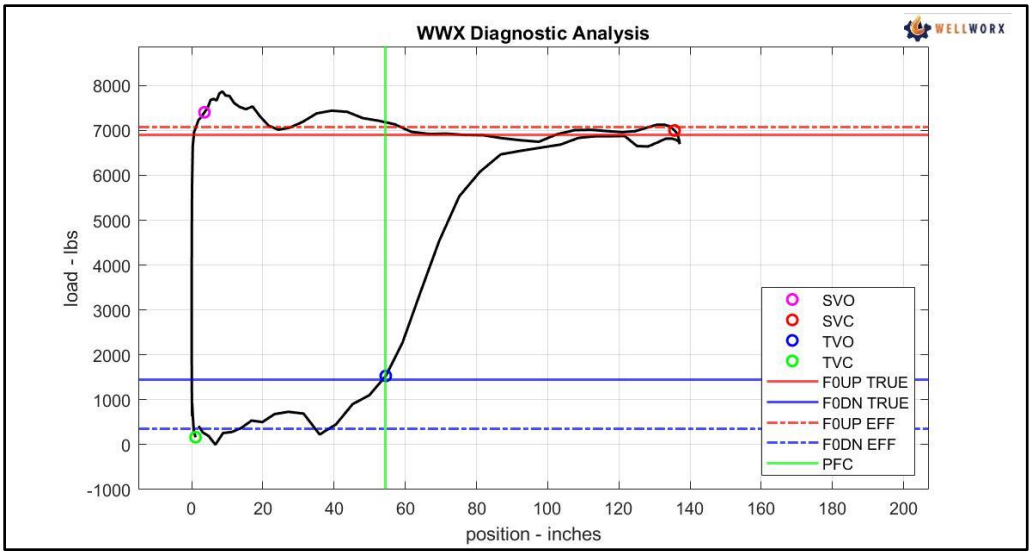

Figure 7: Results of WWX Diagnostic Analysis for Well 1 using ITEDAMP.

WellWorx Diagnostic Report	Well 1 – ITEDAMP	Well 1 – Low Damping (controller)
Surface Stroke Length	126.0 inches	126.0 inches
Speed	12.55 SPM	12.55 SPM
Netstroke	54.52 inches	62.81 inches
Production Rate	319.9 BPD	367.71 BPD
Fluid Load	5453 lbs.	7164 lbs.
Load Range	7870 lbs.	10498 lbs.
Polished Rod Horsepower	33.03 HP	33.03 HP
Pump Horsepower	15.11 HP	30.34 HP
Friction Energy Lost	17.92 HP	2.69 HP
Over - Estimated Production* (24hr)		47.81 BPD/ day pr 1,434 BPD/mth

Table 1: Computed horsepower inferred production and over-estimated production comparison between Well 1 with ideal damping factors and lower damping factors as seen in fixed damping controllers.

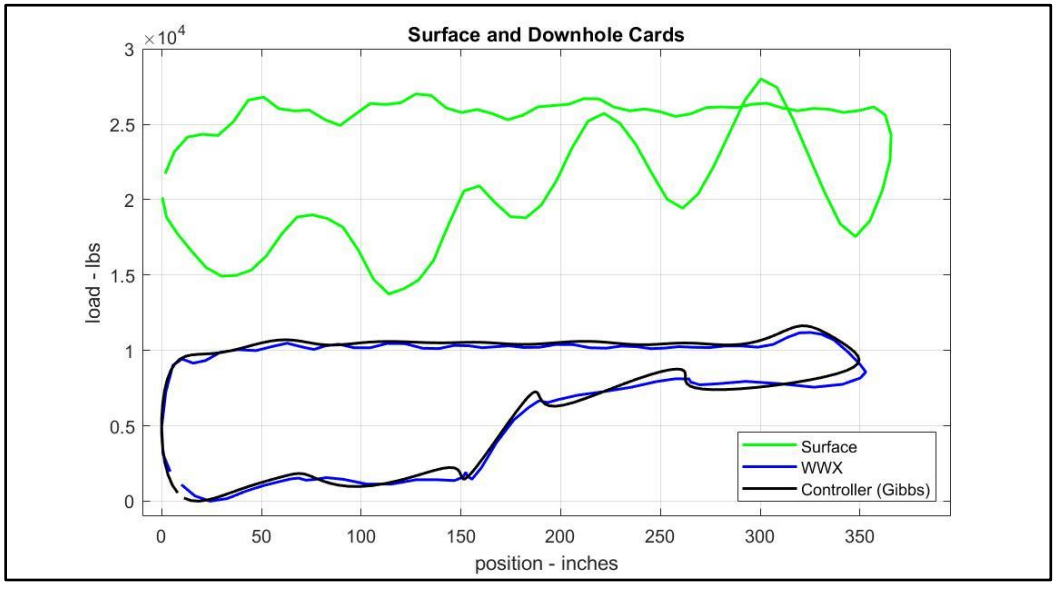

Figure 8: Comparison of results of Iteration on Damping with fixed damping controller method and surface data for Well 2 with low damping factor to match controller output.

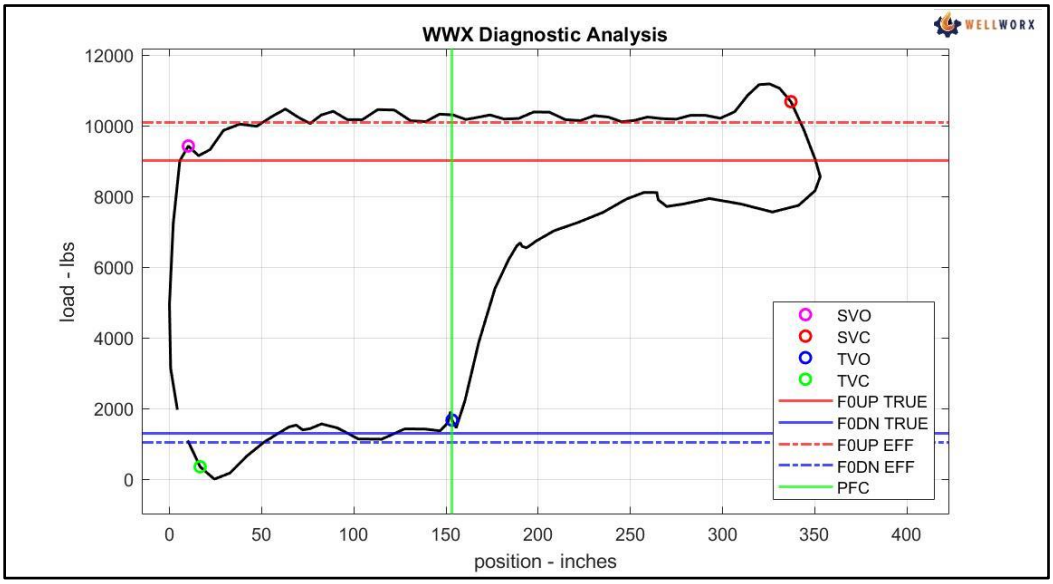

Figure 9: Results of WWX Diagnostic Analysis for Well 2 with low damping factor to match controller output.

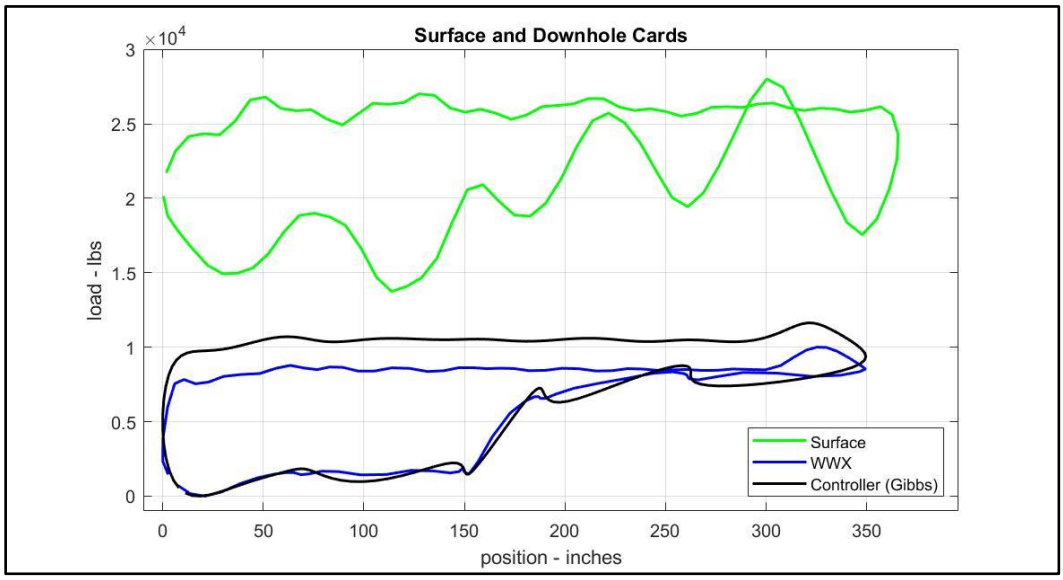

Figure 10: Comparison of results of Iteration on Damping with fixed damping controller method and surface data for Well 2.

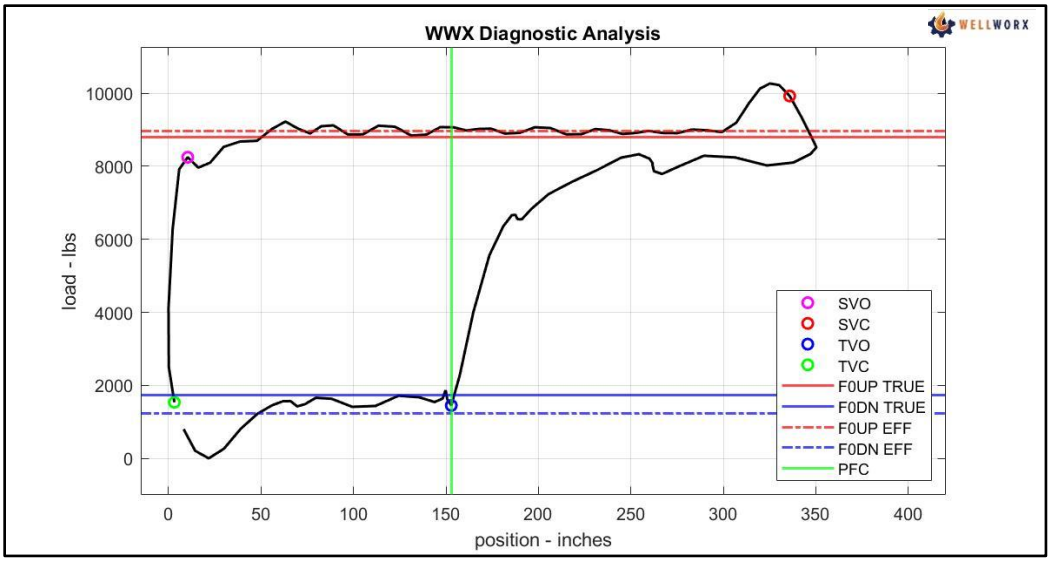

Figure 11: Results of WWX Diagnostic Analysis for Well 2 using ITEDAMP.

WellWorx Diagnostic Report	Well 2 – ITEDAMP	Well 2 – Low Damping (controller)
Surface Stroke Length	366.0 inches	366.0 inches
Speed	3.12 SPM	3.12 SPM
Netstroke	152.08 inches	153.67 inches
Production Rate	221.14 BPD	223.13 BPD
Fluid Load	7306 lbs.	8008 lbs.
Load Range	10002 lbs.	11186 lbs.
Polished Rod Horsepower	17.13 HP	17.13 HP
Pump Horsepower	10.57 HP	15.81 HP
Friction Energy Lost	6.56 HP	1.32 HP
Over - Estimated Production* (24hr)		2 BPD/ day pr 60 BPD/mth

Table 2: Computed horsepower inferred production and over-estimated production comparison between Well 2 with ideal damping factors and lower damping factors as seen in fixed damping controllers.

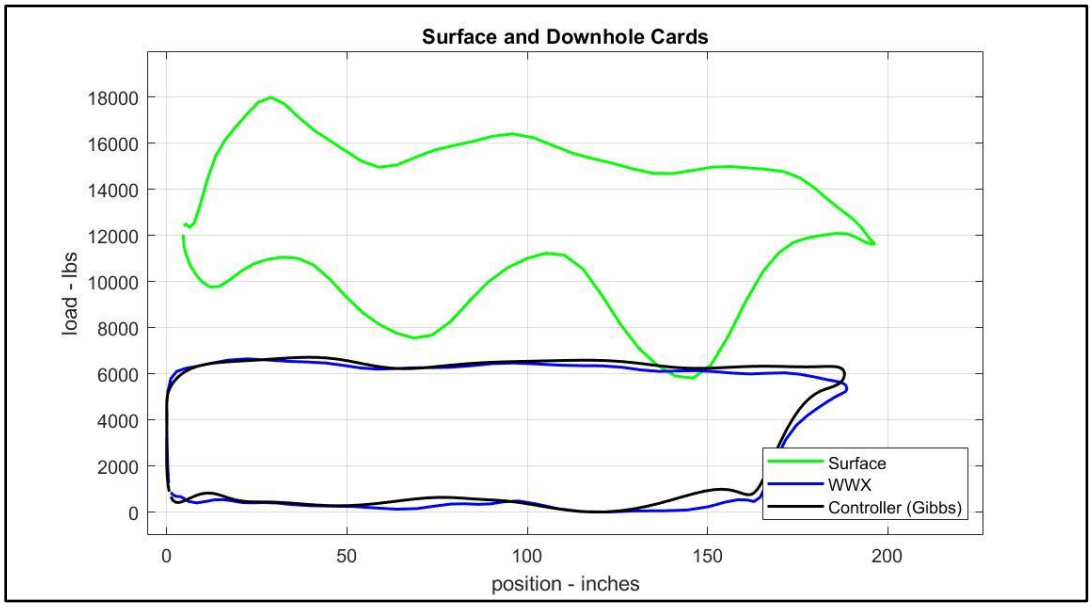

Figure 12: Comparison of results of Iteration on Damping with fixed damping controller method and surface data for Well 3 with low damping factor to match controller output.

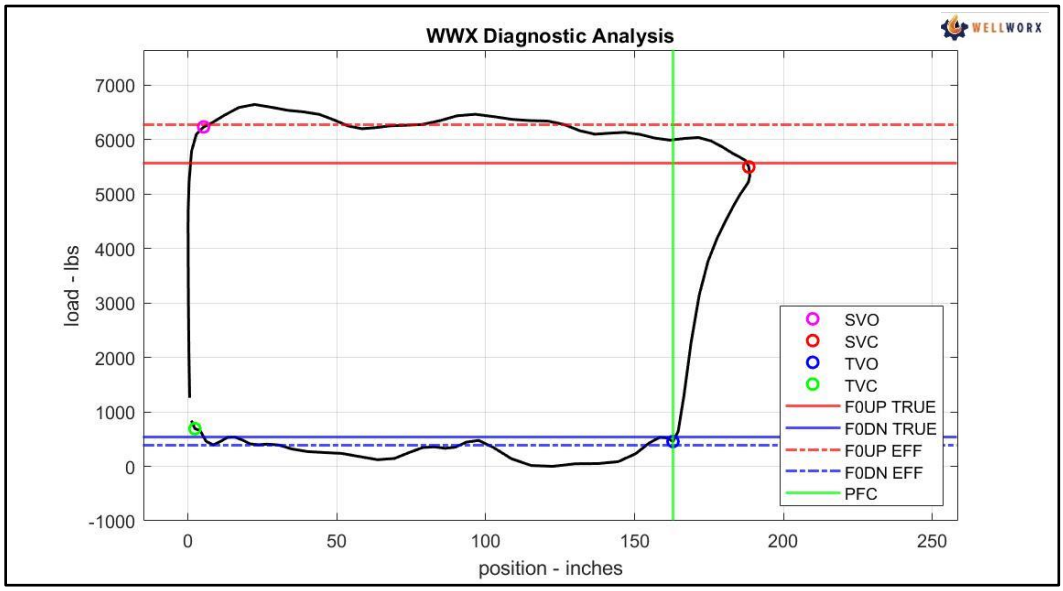

Figure 13: Results of WWX Diagnostic Analysis for Well 3 with low damping factor to match controller output.

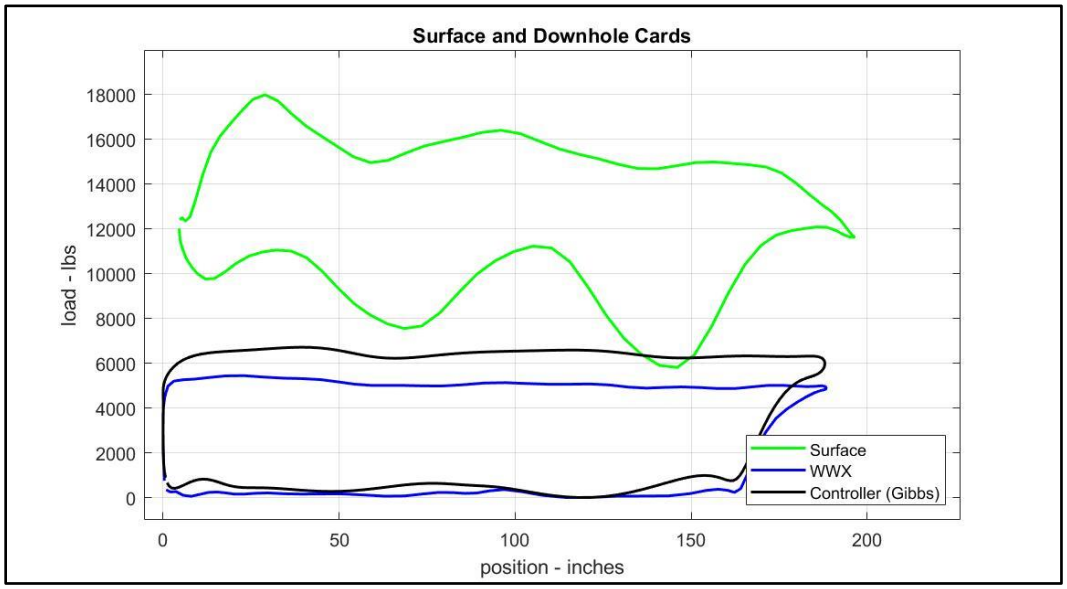

Figure 14: Comparison of results of Iteration on Damping with fixed damping controller method and surface data for Well 3.

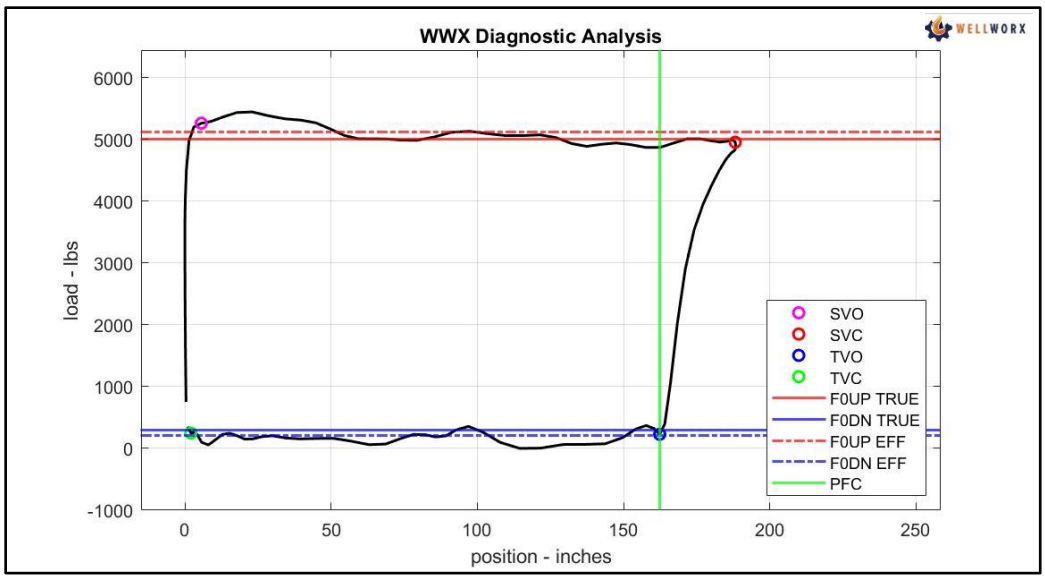

Figure 15: Results of WWX Diagnostic Analysis for Well 3 using ITEDAMP.

WellWorx Diagnostic Report	Well 3 – ITEDAMP	Well 3 – Low Damping (controller)
Surface Stroke Length	192.0 inches	192.0 inches
Speed	6.99 SPM	6.99 SPM
Netstroke	162.33 inches	162.89 inches
Production Rate	529.07 BPD	530.90 BPD
Fluid Load	4706 lbs.	5015 lbs.
Load Range	5443 lbs.	6644 lbs.
Polished Rod Horsepower	19.45 HP	19.45 HP
Pump Horsepower	15.03 HP	18.50 HP
Friction Energy Lost	4.42 HP	0.95 HP
Over - Estimated Production* (24hr)		2 BPD/ day pr 60 BPD/mth

Table 3: Computed horsepower inferred production and over-estimated production comparison between Well 3 with ideal damping factors and lower damping factors as seen in fixed damping controllers.